

## Removal of Cobalt Ions from Aqueous Solutions by Using Poly(*N,N*-dimethylaminopropyl methacrylamide/itaconic acid) Hydrogels

Nalan Baş,<sup>1</sup> Arzu Yakar,<sup>1</sup> Nursel Pekel Bayramgil<sup>2</sup>

<sup>1</sup>Faculty of Engineering, Department of Chemical Engineering, AfyonKocatepe University, Afyonkarahisar, 03200, Turkey

<sup>2</sup>Faculty of Science, Department of Chemistry, Hacettepe University, Ankara, 06800, Turkey

Correspondence to: A. Yakar (E-mail: ayakar@aku.edu.tr)

**ABSTRACT:** In this study, *N,N*-dimethylaminopropyl methacrylamide (DMAPMAM) homopolymer and DMAPMAM/itaconic acid (DMAPMAM/IA) copolymers were obtained from <sup>60</sup>Co- $\gamma$  radiation polymerization. Gel fraction and percentage of swelling values were calculated through gravimetric calculations. In order to increase the swelling of the hydrogel, the amount of IA in initial copolymer composition was gradually increased, but it was observed that gelation values were low. The structural and morphological assessments of homopolymer and copolymers were made by means of several techniques including Fourier Transform Infrared Spectroscopy (FT-IR), Scanning Electron Microscopy (SEM), and Energy-Dispersive X-ray Spectroscopy (EDS). The cobalt ion (Co<sup>2+</sup>) removal capacities of hydrogel were investigated by taking into account of the initial metal ion concentration and pH of aqueous medium. When it came to the maximum capacity of values obtained from adsorption experiments by using Co<sup>2+</sup> solutions at pH 5, they changed between 220 and 245 mg Co<sup>2+</sup>/g dry hydrogel. FT-IR, SEM, EDS, and XRD analyses were carried out for enlightening the mechanism of Co<sup>2+</sup> removal by hydrogels after the completion of adsorption. Also, desorption studies were conducted using ethylenediaminetetraacetic acid (EDTA). Finally, within approximately 5 days, all adsorbed Co<sup>2+</sup> ions were released from hydrogels at pH 5 using 0.1M EDTA solution. © 2013 Wiley Periodicals, Inc. *J. Appl. Polym. Sci.* **2014**, *131*, 39569.

**KEYWORDS:** adsorption; gels; synthesis and processing; swelling; copolymers

Received 29 June 2012; accepted 16 May 2013

DOI: 10.1002/app.39569

### INTRODUCTION

Because of the fact that the world has been experiencing a rapid increase in population and some advances in technology, the need for better quality and high-performance materials has increased. Considering this issue, it calls to mind the fact that polymers are one of the fastest developing materials. A special class of cross-linked polymer, hydrogels are used in many fields such as biomedicine, bioengineering, pharmaceutical, veterinary, food, chemistry, agriculture, and environment, as a result of their biocompatibility and various responses (swelling, shrinkage, etc.) to the external factors (pH, temperature, electrical field, etc.) in the aqueous environment.<sup>1–12</sup> The most threatening problem with which the world has been dealing recently is the environmental pollution that the developing technology has brought about. One source of this kind of environmental pollution—in fact the most prominent factor—is the metals, whose ions and compounds containing toxic properties and which can be seen in the nature, i.e., in sea, river, and lake waters, largely because of the industrial wastes. Certain industrial areas that are effective in directly scattering metals into the environment,

which results in environmental pollution, are cement, iron and steel, chemicals, metals, coal, power plants, textile and agricultural enterprises, and the waste water plants.<sup>13</sup> More seriously, with the mixture of heavy metals with industrial waste water or drinking water, many people and animals are threatened as they accelerate precipitation of proteins in cells, which means a difficulty in breathing and so a decrease in oxygen consumption.<sup>13</sup>

As for the solution, the removal of environmental pollutants such as toxic metals, organic and inorganic compounds from waste waters is such a necessity that can be accomplished through the use of physical, chemical, and biological methods.<sup>14</sup> On the other hand, for the purpose of removing metal ions from various environments, the method that is frequently employed is adsorption. As an adsorbent, hydrogels are successfully applied for the removal of pollutants from aqueous solution as they are easily applicable, have high removal capacity and can be regenerated easily.<sup>15–17</sup> The functional groups such as carboxyl and amino groups on the surface of the hydrogels play a significant role in specifying availability, efficiency, particularity, and reusability of the hydrogel materials in the

adsorption process.<sup>18–21</sup> For this reason, hydrogels containing amine<sup>20–24</sup> and carboxylic acid<sup>25–29</sup> can be given as the most studied hydrogels in the field of adsorption. N,N-dimethylamino-propyl methacrylamide (DMAPMAm) and its copolymers are not widely studied polymers for adsorption process. Çaykara et al. studied with the poly [(N-(3-(dimethylaminopropyl methacrylamide)-co-(lauryl acrylate))] [P(DMAPMA-co-LA)] hydrogels as a function of temperature in aqueous solutions of the sodium dodecyl sulfate (anionic surfactant) and the dodecyltrimethylammonium bromide (cationic surfactant).<sup>30</sup> Tuncel et al. synthesized N-isopropylacrylamide-co-N-[3-(dimethylamino) propyl]methacrylamide (NIPA-co-DMAPMA) copolymers through solution polymerization method. After the experimental results, they investigated that NIPA-co-DMAPMA copolymer could be utilized as a new reagent for the determination of albumin concentration in the aqueous medium.<sup>31</sup> Das et al. prepared a series of new hydrogel (PADMAs) membranes with different compositions of acrylic acid and N-[3-(dimethylamino) propyl]-methacrylamide through aqueous copolymerization, without using chemical crosslinker or radiation. After some characterization analyses and *in vitro* biological tests applied to PADMAs membranes, they observed that membrane composition arranges both pore size and drug diffusion.<sup>32</sup>

In this study, some specific hydrogels called DMAPMAm homopolymer and DMAPMAm/itaconic acid (DMAPMAm/IA) copolymers (synthesized in this study for the first time) were specially prepared and characterized structurally and morphologically by using various methods [Fourier Transform Infrared Spectroscopy (FT-IR), Scanning Electron Microscopy (SEM), Energy-Dispersive X-ray Spectroscopy (EDS), etc.). Next, their Co<sup>2+</sup> adsorption behaviors were investigated by means of solutions having different pH and initial metal ion concentration. Meanwhile, desorption of metal ions were also examined via ethylenediaminetetraacetic acid (EDTA) solution in order to be able to determine the reusability of hydrogels.

## MATERIALS AND METHODS

### Synthesis of Hydrogels

Primarily, DMAPMAm (Sigma-Aldrich Chemie, GmbH, Germany) was directly placed into PVC straws and irradiated in different doses in air at ambient temperature in a Gammacell-220 type radiation source at a fixed dose rate of 1.5 kGy/day. The synthesis of DMAPMAm/IA copolymers was conducted by following the same procedure as the previous hydrogel except one difference in which it included 1, 5, and 10 mg IA (Merck, Darmstadt, Germany).

As for the procedure, first of all, samples irradiated in various doses in PVC straws were removed from pipette and cut into 2–3 mm long pieces. Later, they were dried in air and then in a vacuum oven held at 30°C. After that, they were weighed to obtain  $w_0$  value. For the removal of residual monomers and/or uncross-linked polymer chains in the structures, these weighed hydrogels were soaked in water and then once again hydrogels were dried in air and in a vacuum oven and re-weighed ( $w$ ). Gel fraction (%) values were calculated by using the following equation:

$$\text{Gelation (\%)} = \frac{w}{w_0} \times 100 \quad (1)$$

### Characterization of Hydrogels

The structural characterization of both homo and copolymers and their adsorbed state was accomplished by using FT-IR and SEM analysis methods. In order to identify formations occurring on the polymer surfaces, XRD analyses were carried out. Later, FT-IR spectra of hydrogels were recorded with Perkin Elmer Spectrophotometer and collected for 10 scans at a 4 cm<sup>-1</sup> resolution in the range of 4000–400 cm<sup>-1</sup>. As the next step, SEM images and EDS surface analysis was carried out by using a Bruker Electron Microscope so that it could be possible to observe morphological changes in an accelerating voltage of 15.00 kV. Polymer samples were coated in gold as they required to be conductive. After that, with the XRD patterns taken by Rigaku D-MAX 200 X-ray diffractometer, XRD analysis was carried out in the range from about 10° to about 90° 2θ CuKα.

### Determination of Swelling (%) Values

Initially in this phase, preweighed dry hydrogels were immersed in de-ionized water and phosphate buffer solutions of pH ranging from 3 to 10. The process was as follows: The swollen gels removed from the de-ionized water (or buffer solutions) at certain time intervals were dried superficially with filter paper, weighed, and placed in the same solution. As a follow-up, the measurements were repeated until they swelled equally. Swelling (%) values were calculated through following equation:

$$\text{Swelling (\%)} = \frac{w_t - w_0}{w_0} \times 100 \quad (2)$$

where  $w_0$  stands for the weight of dry gel,  $w_t$  stands for the weight of swollen gel at a specific time  $t$ .

### Adsorption of Metal Ions

Metal ion solutions used in adsorption experiments were prepared with CoCl<sub>2</sub>·6H<sub>2</sub>O purchased from BDH, England. For the purpose of analyzing the effect of initial metal ion concentration on adsorption, Co<sup>2+</sup> solutions having pH 3 and pH 5 of phosphate buffer solutions within the concentration range of 500–1750 mg/L were used. Because of the presence of large amounts of phosphate in waste water, phosphate buffer solution was used as an aqueous solution in the study. In the next phase, some certain amount of hydrogel was immersed in 10 mL of Co<sup>2+</sup> solution and kept at 25°C until the equilibrium value was attained. The measurement of initial and equilibrium concentrations was conducted through the usage of Shimadzu 1601 model UV-Vis spectrophotometer. The Co<sup>2+</sup> adsorption capacity was determined by measuring the initial and final concentrations of Co<sup>2+</sup> in the adsorption medium spectrophotometrically at 510 nm that was the maximum adsorption wavelength of Co<sup>2+</sup> and equilibrium adsorption values were calculated by using the following equation:

$$q_e = \frac{(C_0 - C_e) \times V}{m} \quad (3)$$

where  $q_e$  is the the amount of Co<sup>2+</sup> adsorbed by hydrogel (mg/g);  $C_0$  the initial Co<sup>2+</sup> concentration of solution (mg/L);  $C_e$  the equilibrium concentration of Co<sup>2+</sup> remaining in solution after adsorption (mg/L);  $m$  the weight of dry gel (g); and  $V$  the volume of solution (L).

In order to monitor the adsorption kinetics, 0.04 g of hydrogel was placed into 1000 mg/L  $\text{Co}^{2+}$  solution and pH value was adjusted to 3 and 5 with phosphate buffer. Samples were taken periodically from the solution to determine the equilibrium concentration of  $\text{Co}^{2+}$  by using UV-Vis spectrophotometer.

### Desorption of Metal Ions

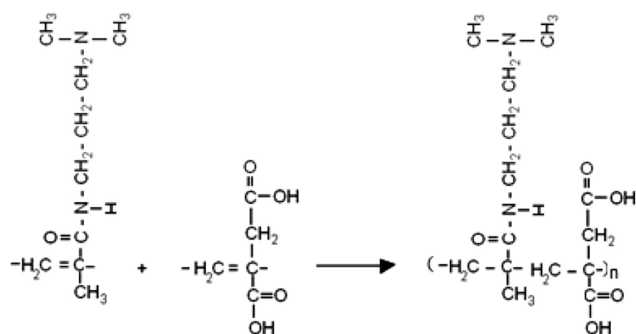
For the desorption studies, 0.1M EDTA solution was used. Here in this part, while  $\text{Co}^{2+}$  adsorbed hydrogels were kept at pH 3 and 5 of EDTA solution, the concentration of released metal ions was measured at regular intervals by using Shimadzu 1601 UV-Vis spectrophotometer. Desorption (%) values were calculated by means of the following equation:

$$\text{Desorption (\%)} = \frac{\text{amount of released metal ions}}{\text{total amount of adsorbed metal ions}} \times 100 \quad (4)$$

## RESULTS AND DISCUSSION

### Synthesis of Hydrogels

DMAPMAM and its solutions with IA (1, 5, and 10 mg) were irradiated with a  $^{60}\text{Co}$ - $\gamma$  source, and homo- and co-polymeric hydrogels were obtained. The reaction between the monomers is given below.



Their gelation percentage-dose curves are shown in Figure 1. It can be concluded from this figure that gel fraction (%) values increase with the increasing amount of applied dose and reach the maximum values (approximately 100%) at 25 kGy dose.

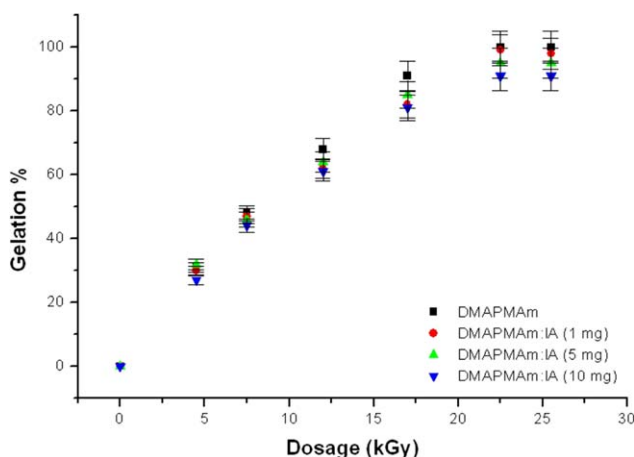


**Figure 1.** The effect of dose amounts on gel fraction. [Color figure can be viewed in the online issue, which is available at [wileyonlinelibrary.com](http://wileyonlinelibrary.com).]

**Table I.** Density of Hydrogels

Gel system	<i>d</i> (g/mL)
DMAPMAM	0.9475
DMAPMAM:IA (1 mg)	0.9126
DMAPMAM:IA (5 mg)	0.8748
DMAPMAM:IA (10 mg)	0.8784

Moreover, there is a slight decrease in the gel fraction with the increase in IA content in the studied range. The reason of this can be explained with IA that serves as chain transfer agent causing decrease in the amount of crosslinks.<sup>33</sup> Regardless of the initial IA content, 25 kGy irradiated samples were later used for swelling and adsorption experiments. To get an idea about the impact of the amount of IA on the pore structure of the hydrogel, density measurements were made by means of pycnometer at room temperature using benzene as a solvent. Results are given in Table I. As seen in Table I, density values decrease beginning from the pure polyDMAPMAM to poly(DMAPMAM/IA) hydrogel including high amount of IA and thus the polymer density, i.e., the number of polymer segments in the hydrogel structure decrease. It is thought that this decrease causes a decrease in the crosslink density.<sup>34</sup>

### FT-IR Characterization of Hydrogels

FT-IR spectra of pure polyDMAPMAM and poly(DMAPMAM/IA) hydrogel are given in Figure 2. Thoroughly examination of the figure indicates clearly that the peak intensity in the spectra of poly (DMAPMAM/IA) (5, 10 mg) was increased with the increasing amount of IA. In addition, bands at 3200–3600 and 1700  $\text{cm}^{-1}$  are noteworthy. It is known that bands at 1725, 1700, and 1650  $\text{cm}^{-1}$  are defined as symmetric and antisymmetric stretching vibrations of carbonyl groups in the acid type substances and carbonyl group in the amide type substance, respectively.<sup>33</sup> A broad band, which is seen at 3200–3600  $\text{cm}^{-1}$ , shows the presence of O-H bonding in the structure, whereas band observed at 2900  $\text{cm}^{-1}$  is defined as alkyl groups C-H stretching. On the other hand, band at 1550  $\text{cm}^{-1}$  shows that there may be –OH and –NH stretching that have attached to the carbonyl group in the structure. Whereas the band at 1400  $\text{cm}^{-1}$  shows the presence of (–CH<sub>2</sub>–) group on the side chain, band at 1200  $\text{cm}^{-1}$  refers to C–N stretching.<sup>35</sup> As clearly seen from the spectrum of poly(DMAPMAM/IA (1 mg)) hydrogel, the presence of different C = O bands observed at 1700 and 1650  $\text{cm}^{-1}$  shows both the amide and acid group contributions to poly (DMAPMAM/IA) hydrogels. Less notable changes in the FTIR spectra of the copolymers are because of the fact that small amount of IA has been added to the polyDMAPMAM structure. Furthermore, when more IA has been added to the structure, it has served as a chain transfer agent and has modified the form of hydrogel.

### Swelling Studies

In order to make clear the mechanism of solvent diffusion to 3-D network structure of the gel, determination of the swelling behavior of hydrogel is essential. The examination of the swelling behaviors of both polyDMAPMAM and poly(DMAPMAM/

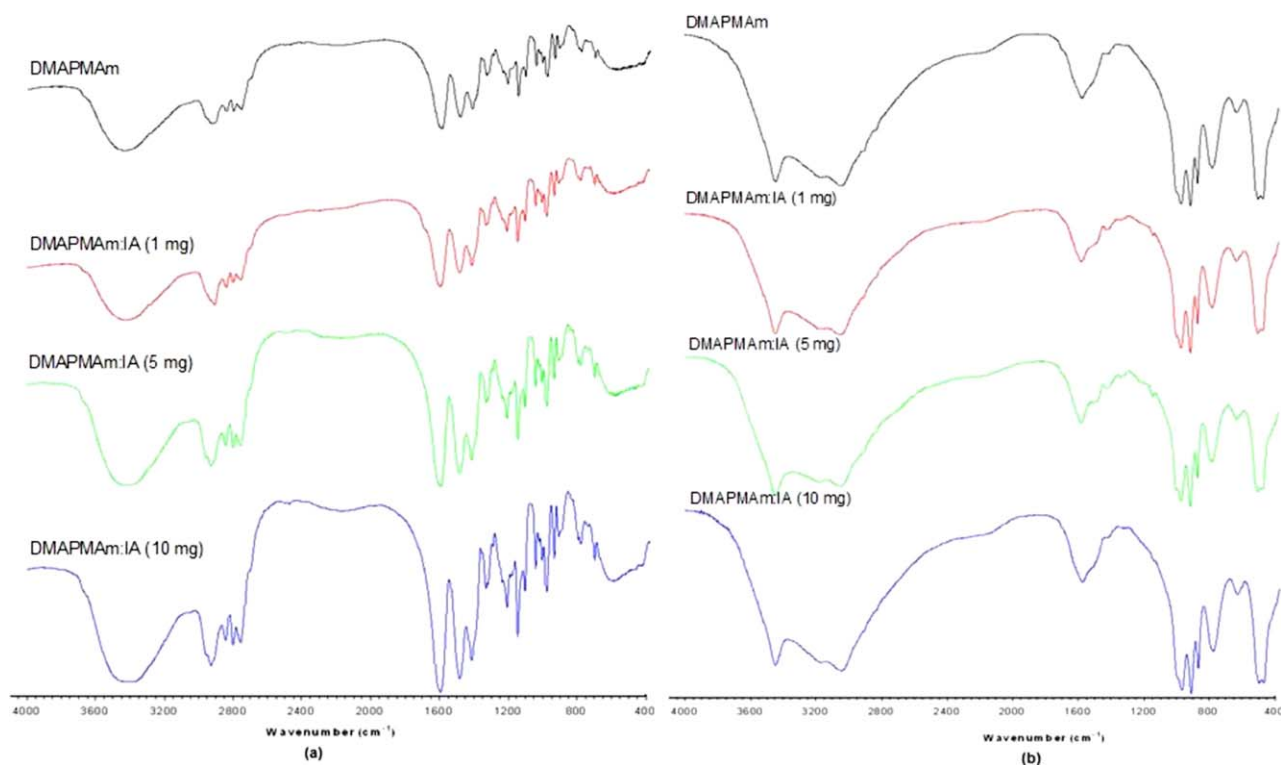


**Figure 2.** FTIR spectra of hydrogels: (a) before adsorption and (b) after  $\text{Co}^{2+}$  adsorption. [Color figure can be viewed in the online issue, which is available at [wileyonlinelibrary.com](http://wileyonlinelibrary.com).]

IA) hydrogel reveals that they do not lose their homogeneous appearance during swelling. At the end of the swelling, both of the hydrogel systems retain their geometric shape, which they have in the dry state. The swelling percentage–time plots drawn by data obtained from swelling studies of hydrogel in de-ionized water can be seen in Figure 3. The figure demonstrates that swelling percentage values of hydrogel reach a limiting value, which is the equilibrium value within 2800 min. The important point in swelling curves is the fact that the more IA content there is in the gel system, the more swelling (%) value there is. Therefore, incorporation of IA into polyDMAPMAm

structure causes an increase in the number of ionizable groups, leading to a decrease in the density of cross-links in gel system. Thus, it has been possible to add more water molecules to the network structure resulting from the electrostatic repulsion between the ionizable groups. In addition, these conclusions are supported by gel fraction–dose curves and the density values of hydrogel (Figure 1 and Table I).

After that, the hydrogel samples were placed into phosphate buffer solutions with pH 3 to 10 at  $25^\circ\text{C}$  to investigate the swelling behaviors at various pHs. In Figure 4 showing the pH–

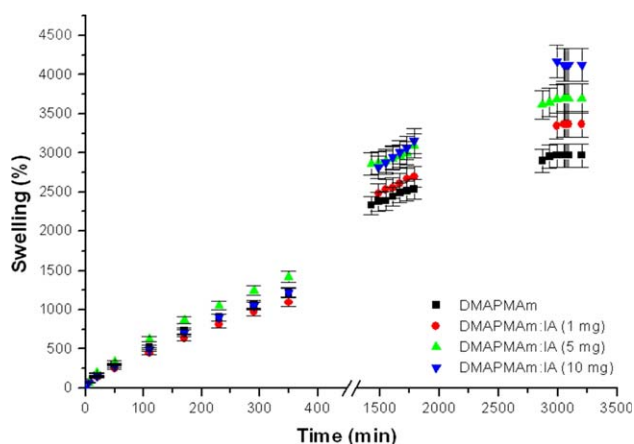


**Figure 3.** Swelling properties of hydrogels depend on time. [Color figure can be viewed in the online issue, which is available at [wileyonlinelibrary.com](http://wileyonlinelibrary.com).]

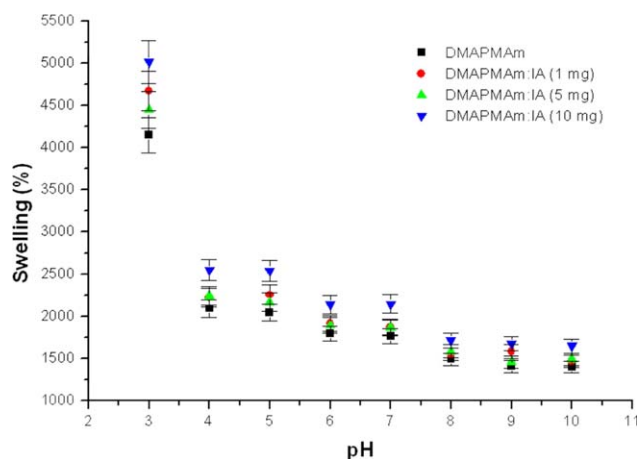


**Figure 4.** Effect of pH on the equilibrium degree of swelling of hydrogels. [Color figure can be viewed in the online issue, which is available at [wileyonlinelibrary.com](http://wileyonlinelibrary.com).]

dependent swelling behaviors of the completely swollen hydrogels, it is observed that hydrogels have high swelling values in acidic pHs. While the maximum swelling values of hydrogels at pH 4 and pH 5 are almost the same (approximately swelling (%) value 2500), the maximum swelling value at pH 3 has suddenly increased and reached to 4000–5000 values. In addition, swelling value of poly (DMAPMAM/IA) hydrogels increases with the increasing amount of IA, even with very small differences. The explanation for the present results is as follows: as IA contains two carboxylic acid groups, it has two ionization constants ( $K_{a1} = 1.40 \times 10^{-4}$ ,  $K_{a2} = 3.56 \times 10^{-6}$ ).<sup>35</sup> Consequently, poly (DMAPMAM/IA) hydrogels are both acidic (-COOH) and basic (-NH-) in nature. On the other hand, -NH groups of DMAPMAM are well protonated to form  $-\text{NH}_2^+$  in the acidic region, which leads to an increase in swelling value because of  $-\text{NH}_2^+ -\text{NH}_2^+$  repulsions. However, after pH 5, no significant increase in the value of swelling has been observed as the very small amount of IA contributes to DMAPMAM structure. Adsorption studies have been performed in the solutions containing pH of 3, 4, and 5, which are the admissible value of swelling, so as to provide dimensional stability.

#### Adsorption Studies

The effect of adsorbent amount on adsorption was previously investigated. With this purpose, adsorption behavior of gels were examined in the  $\text{Co}^{2+}$  ion solutions having 1000 mg/L metal ion concentration and pH 3 and pH 5 by using 0.005, 0.01, 0.02, 0.03, 0.04 g gel. As seen in the pre-experiments that maximum adsorption capacities of gels have not changed too much with the increasing amount of gel, (Data not given) which leads to the selection of 0.04 g gel as the amount of adsorbent. Certain amounts of polyDMAPMAM and poly (DMAPMAM/IA) hydrogels were placed individually in  $\text{Co}^{2+}$  containing solutions of 1000 mg/L for studying the adsorption kinetics. Figure 5 shows that the kinetic of  $\text{Co}^{2+}$  adsorbed by hydrogels has developed so rapidly that 65 mg metal ions per unit weight of gel have been adsorbed within the first 5 min. Approximately 3 h later, although the adsorbed metal per unit mass of gel is about 80 mg at pH 3 solution, this value has risen to 125 mg at pH 5 solution. The time, in which the adsorption reaches the equilibrium, is approximately 25 h. While the rapid diffusion of water into gel structure causes the gels' swelling in a short time thanks to this accelerated adsorption of metal ions, this case has enabled to reach the equilibrium of system in a short time.

In order to investigate the effect of initial metal ion concentration and pH on  $\text{Co}^{2+}$  adsorption, firstly, hydrogels were put into the solutions with concentrations in the range of 500–1750 mg/L. Next, adsorption isotherms were constructed by graphing the amount of adsorbed  $\text{Co}^{2+}$  (mg) per g of dry hydrogel in equilibrium versus  $\text{Co}^{2+}$  solution concentrations (mg/L) remaining in the solution in equilibrium. The adsorption isotherms are given in Figure 6 for the solutions of pH 3, pH 4, and pH 5, respectively. The common characteristics of all these isotherms are that they have increased rapidly at first adsorption, and then reached a plateau region and finally remained constant even if the concentration of  $\text{Co}^{2+}$  solution has been increased further. A possible reason is that the surface has been filled completely with adsorbed molecules, that is, the  $\text{Co}^{2+}$

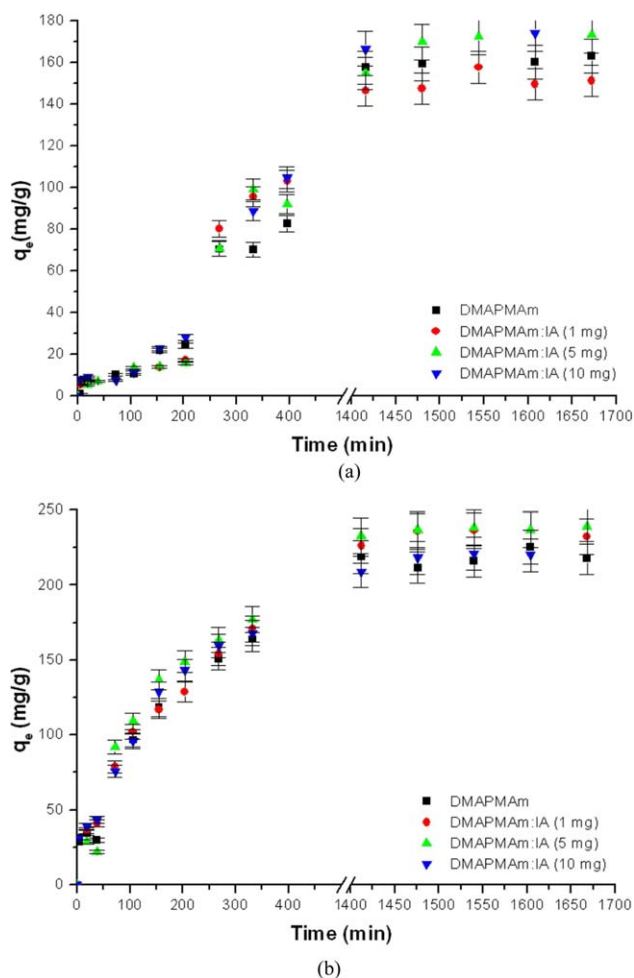


**Figure 5.** Adsorption kinetics of hydrogels: (a) at pH 3 and 1000 mg/L  $\text{Co}^{2+}$  solution, and (b) at pH 5 and 1000 mg/L  $\text{Co}^{2+}$  solution. [Color figure can be viewed in the online issue, which is available at [wileyonlinelibrary.com](http://wileyonlinelibrary.com).]

adsorption on hydrogels has been higher in low concentrations, yielding Langmuir-type isotherms. Langmuir isotherm is often observed in the adsorption from solution.<sup>36</sup>

As can be seen in Figure 6, maximum  $q_e$  values obtained at pH 3 are changed from 185 to 200 mg  $\text{Co}^{2+}$  ion/g gel according to the gel composition. When the adsorption experiments are made with  $\text{Co}^{2+}$  solutions that are prepared with pH 4 buffer solutions, maximum  $q_e$  values have been changed from 203 to 219 mg/g values. Higher  $q_i$  values (219–245 mg/g) have been obtained by using  $\text{Co}^{2+}$  solutions (at pH 5), which are the ionization of first carboxyl group of IA ( $K_{a1} = 1.40 \times 10^{-4}$ ). At low solution pH values, a comparatively high concentration of protons have been available to protonate amine groups of hydrogels to form  $-\text{NH}_2^+$  groups and to ionize carboxylic acid groups of hydrogels to form  $-\text{COO}^-$ , resulting in an increase in the adsorption of anionic ( $\text{Cl}^-$ ,  $\text{PO}_4^{3-}$  (coming from the buffers)) and cationic ( $\text{Co}^{2+}$ ) groups. On the other hand, the protonation of amine groups leads strong electrostatic repulsion of the cationic metal ions to be adsorbed. However, at higher solution of pH 5 value (lower proton concentrations), less protons

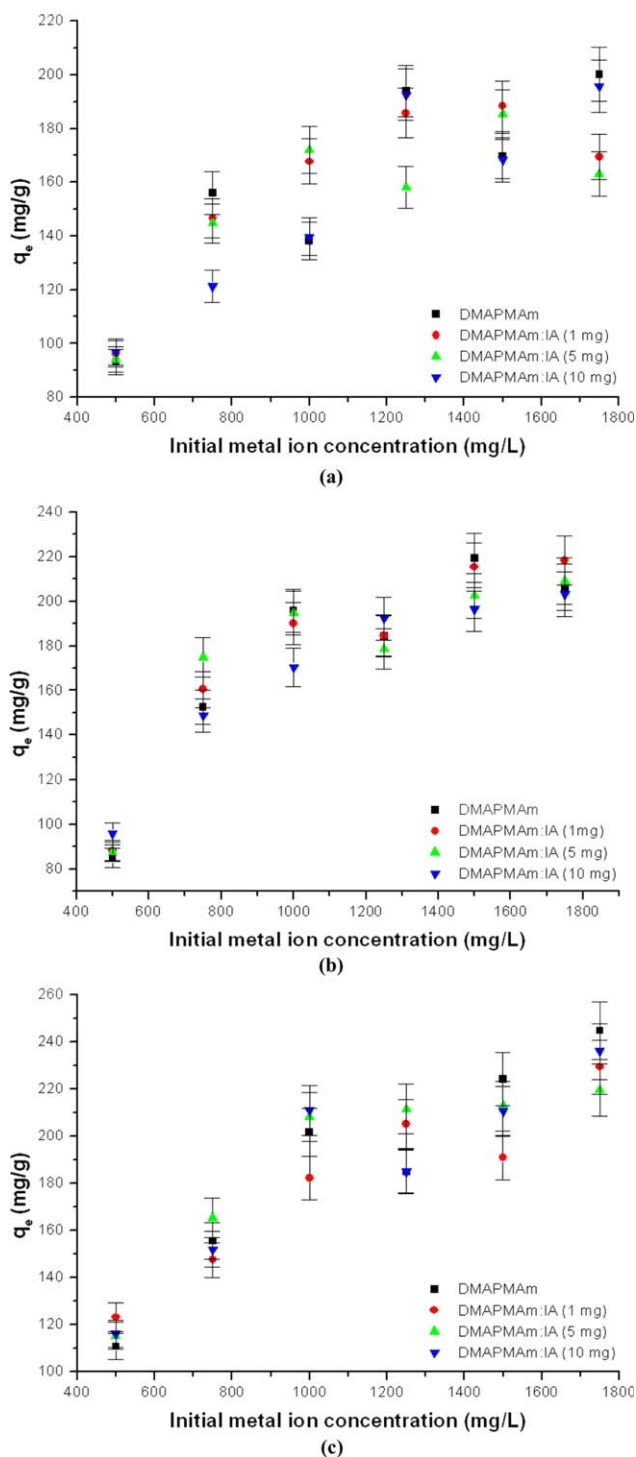


**Figure 6.** Metal adsorption of hydrogels (a) at pH 3  $\text{Co}^{2+}$  solution, (b) at pH 4  $\text{Co}^{2+}$  solution, and (c) at pH 5  $\text{Co}^{2+}$  solution. [Color figure can be viewed in the online issue, which is available at [wileyonlinelibrary.com](http://wileyonlinelibrary.com).]

would be available to protonate  $-\text{NH}$  to form  $-\text{NH}_2^+$ , neutral nitrogen of amine group has a lone pair of electrons that can bind a metal ion through sharing an electrons pair to form a metal complex.<sup>22–24</sup> As a result, metal ions are more favorably adsorbed onto the surfaces of the hydrogels at relative higher pH value.<sup>22</sup> For the same reason, DMAPMAm hydrogel has showed the maximum adsorption behavior against  $\text{Co}^{2+}$  ions.

### FT-IR Characterization of Hydrogels after Adsorption

FT-IR spectra of  $\text{Co}^{2+}$  adsorbed hydrogels are given in Figure 2(b). In comparison with Figure 2(a), Figure 2(b) has differences in terms of FT-IR spectra of hydrogels after  $\text{Co}^{2+}$  adsorption. Broad band at  $3200\text{--}3600\text{ cm}^{-1}$  belonging to  $-\text{OH}$  gets narrow and C-H aliphatic stretching band, which is seen at  $2900\text{ cm}^{-1}$ , expands and gets deformed. Likewise, there has been altered in the band shape because of the gel–metal interactions at  $1550\text{ cm}^{-1}$ , which is attached to the carbonyl group in the structure and originates from  $-\text{OH}$  and  $-\text{NH}$  stretching vibrations. The reason of this can be explained by the strong interactions occurring between  $\text{Co}^{2+}$  ions and functional groups of hydrogels. Therefore, it is possible to come up with the conclusion that the polymer–metal interactions occur between  $\text{Co}^{2+}$  ions and  $-\text{COOH}$  and  $-\text{NH}$  groups of hydrogel. A high level of alteration has occurred at the right-hand side of  $1400\text{ cm}^{-1}$ , defined as the fingerprint region. The bands especially in the  $1100\text{--}500\text{ cm}^{-1}$  range belonging to  $-\text{PO}_4$  functional groups demonstrate that phosphate groups enter the structure.

### Surface Analysis of Hydrogels after Adsorption

The SEM allows for observing topographic features of the materials as three-dimensional images and the EDS fulfils an elemental analysis on microscopic sections of the materials. SEM and EDS data were collected to clarify the morphological changes of hydrogels' surface depending on  $\text{Co}^{2+}$  adsorption. As shown in SEM images given in Figure 7, there can be seen long rod-shaped crystals which are concentrated on some major global regions and occur with interaction of  $\text{Co}^{2+}$  on the surfaces of hydrogels. EDS analysis of hydrogels performed to explain the mechanism of  $\text{Co}^{2+}$  adsorption on hydrogels (Figure 8) shows adsorbed  $\text{Co}^{2+}$  and  $\text{Cl}^-$  ions on hydrogel surface as pink and blue colors, respectively. When the images are thoroughly examined, it is recognized that pink and blue colors are found to be concentrated in certain regions. Also, these colors show the active ends of the polymers when it is taken into account that  $\text{Co}^{2+}$  and  $\text{Cl}^-$  ions interact with the negative ends ( $-\text{COO}^-$ ) and positive ends ( $-\text{NH}_2^+$ ) of the polymers in the acidic pH values, respectively. Additionally, phosphorus can also be observed on the surface of the hydrogels from EDS spectrum. When this result accords with FT-IR analysis, it is thought that negative ends in the Figure 2 have originated from the presence of phosphate groups as both FT-IR and EDS analyses have supported each other. The reason of the degradations seen at the  $-\text{COOH}$  and  $-\text{CH}$  bands in the FTIR spectra is interpreted as the interactions occurring between  $\text{Co}^{2+}$  ions with  $-\text{COOH}$ ,  $-\text{CH}$  functional groups. In addition, reason for the degradation of  $-\text{NH}$  bands seen at the FTIR spectra is thought to be interactions between the  $\text{Cl}^-$  and  $\text{PO}_4^{3-}$  ions with the  $-\text{NH}$  functional groups. Phosphate bands recognized in the FTIR spectra have shown that phosphate groups are adsorbed by the gel surface. In parallel with the analysis of FTIR, Cl, and P atoms have also been detected as well as Co atoms on the gel surface through EDS analyses. While the  $\text{Cl}^-$  ions connect directly to the polymer,  $\text{Co}^{2+}$  ions have formed crystal with the other groups in the structure and thus remained on the polymer surface. Possible adsorption mechanism of  $\text{Co}^{2+}$  metal ion that occurs on the polymer surface at pH 4 and 5 is given below.

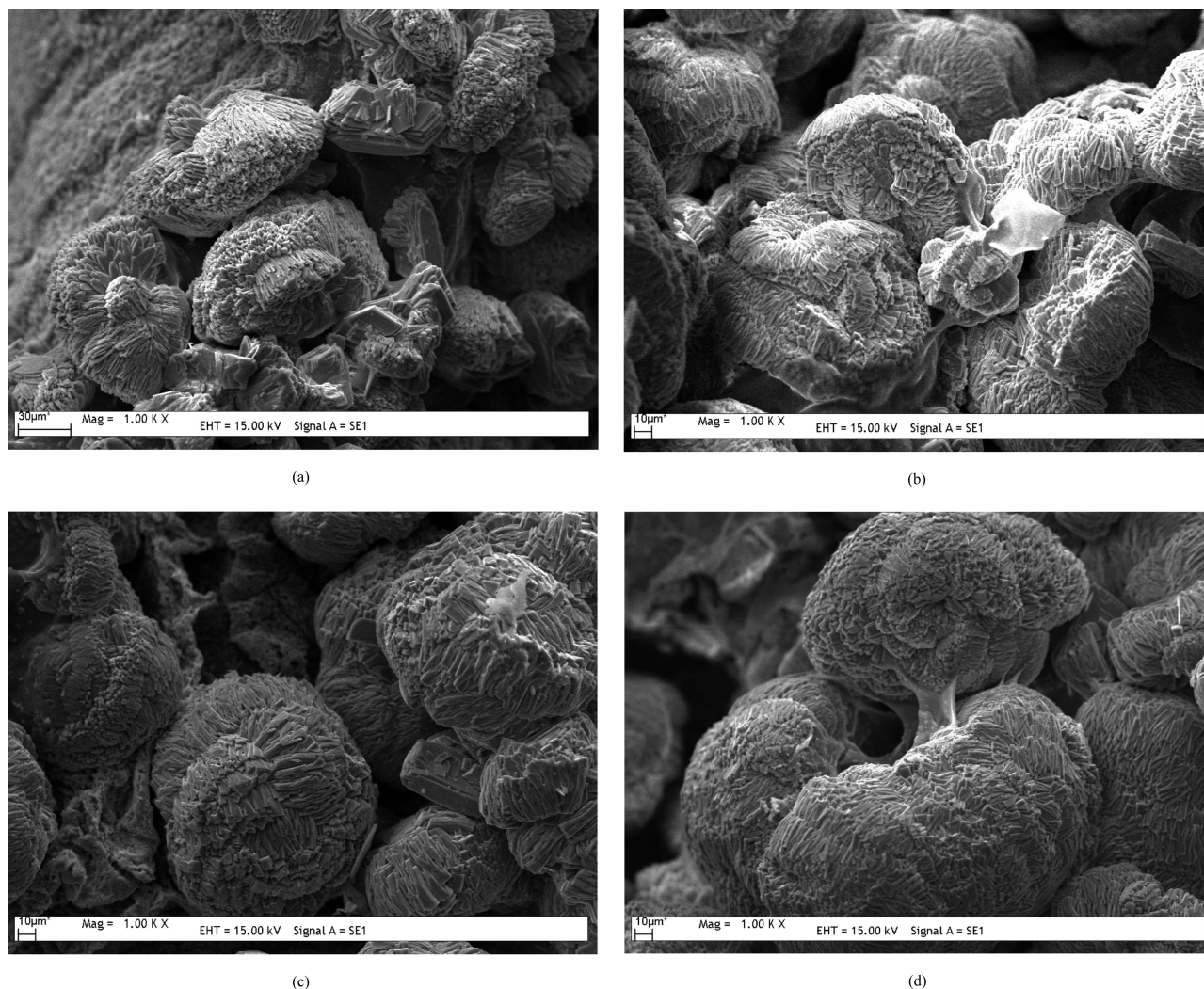
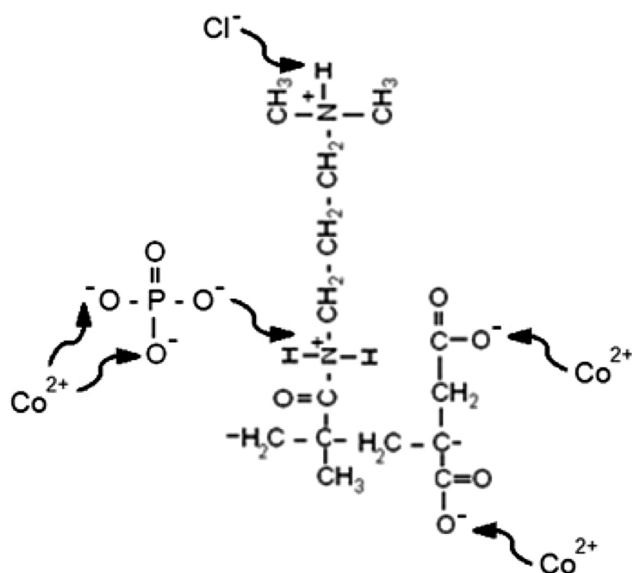


**Figure 7.** SEM images of (a) poly(DMAPMAm), (b) poly(DMAPMAm/IA (1 mg)), (c) poly(DMAPMAm/IA (5 mg)), and (d) poly(DMAPMAm/IA (10 mg)) exposed to 1000 mg/L aqueous  $\text{Co}^{2+}$  solution.



The analysis of XRD performed to identify the crystal structure formed on the polymer surfaces after adsorption (Figure 9) indicates about  $\text{Co}^{2+}$  adsorbed hydrogels that a crystal structure is available. Furthermore, XRD patterns of hydrogels are in agreement with the XRD pattern of cobalt phosphate octahydrate ( $\text{Co}_3(\text{PO}_4)_2 \cdot 8\text{H}_2\text{O}$ ) (Figure 9). Another important point of the XRD data is that they have given parallel results with the FT-IR, SEM, and EDS. Considering all these data together, it has been observed that phosphate ions getting from phosphate buffer solution interact with the cobalt ions by clinging on to the gel, which makes it possible to form cobalt–phosphate crystal on the gel surface.

#### Adsorption Isotherms

The adsorption of  $\text{Co}^{2+}$  on hydrogels was analyzed by using Langmuir<sup>37</sup> and Freundlich<sup>38</sup> isotherms.

The linear form of Langmuir equation is given by eq. (5), where  $K_L$  is the Langmuir adsorption constant (L/mg), which is related to energy of adsorption and also shows the relationship between

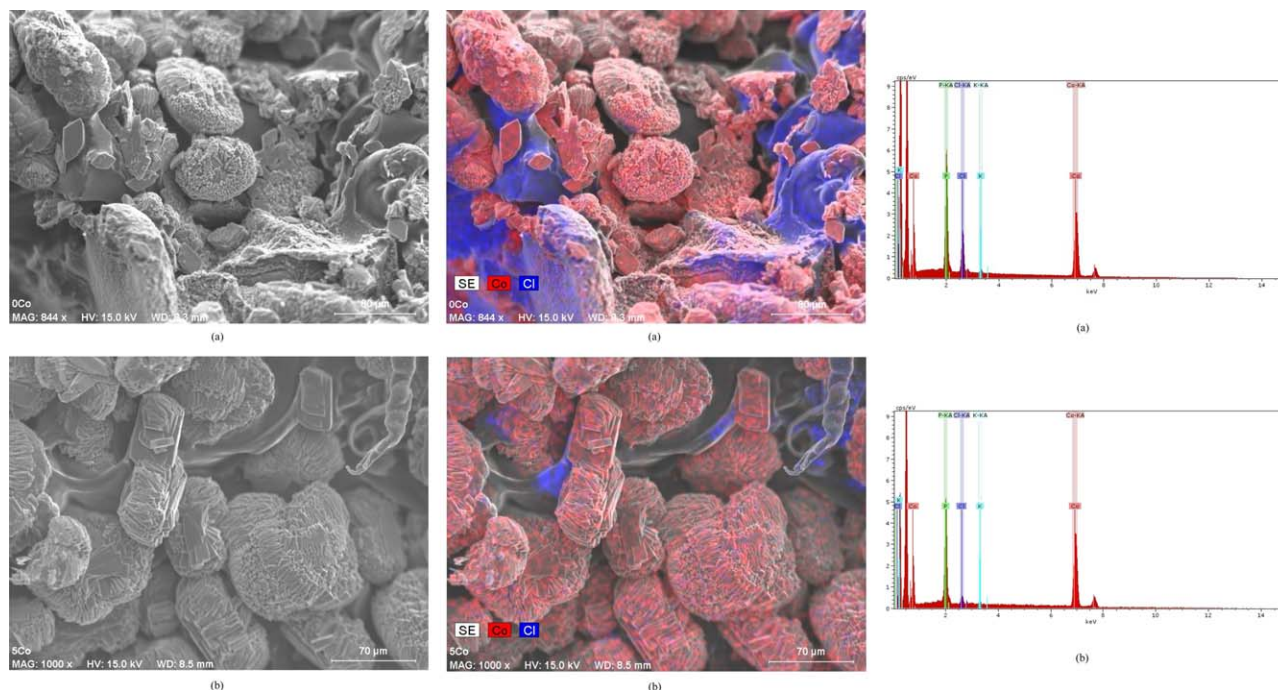


**Figure 8.** EDS analyses of (a) polyDMAPMAm, and (b) poly(DMAPMAm/IA (10 mg)) exposed to 1000 mg/L aqueous  $\text{Co}^{2+}$  solution. [Color figure can be viewed in the online issue, which is available at [wileyonlinelibrary.com](http://wileyonlinelibrary.com).]

adsorbent and adsorbate and  $q_{\max}$  is the adsorption capacity (mg/g) constant.

$$\frac{C_e}{q_e} = \frac{C_e}{q_{\max}} + \frac{1}{K_L \cdot q_{\max}} \quad (5)$$

The rearranged Freundlich equation can be expressed by eq. (6), where  $K_F$  is related to adsorbent capacity and  $1/n$  is the heterogeneity factor ranging from 0 to 1, which shows intensity of adsorption.

$$\log q_e = \log K_F + \frac{1}{n} \log C_e \quad (6)$$

Parameters calculated using eqs. (5) and (6) are given in Table II.  $K_L$  and  $q_{\max}$  were reached from the slope and the intercept of the linear plots of  $C_e/q_e$  versus  $C_e$ , respectively.

Maximum adsorption capacity values obtained from prepared gels are given in Table III in comparison with similar studies in the literature,<sup>39–50</sup> which shows that the synthesized homo- and co-polymers in our work have the highest values.

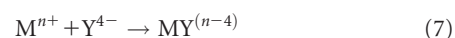
The Langmuir has been developed to explain chemisorption on a homogeneous and distinct localized adsorption sites, indicating no interaction between adjacent molecules. In addition, single coating layer occurs on the adsorption surface during the adsorption process, which makes us to conclude that the experimental data adjust well to Langmuir model and the calculated values are listed in Table II. It can be inferred from this table that calculated  $q_{\max}$  values for hydrogels are considerably similar to the Langmuir values.

The Freundlich isotherm is not just confined to the formation of the monolayer coverage assuming that adsorption occurs on

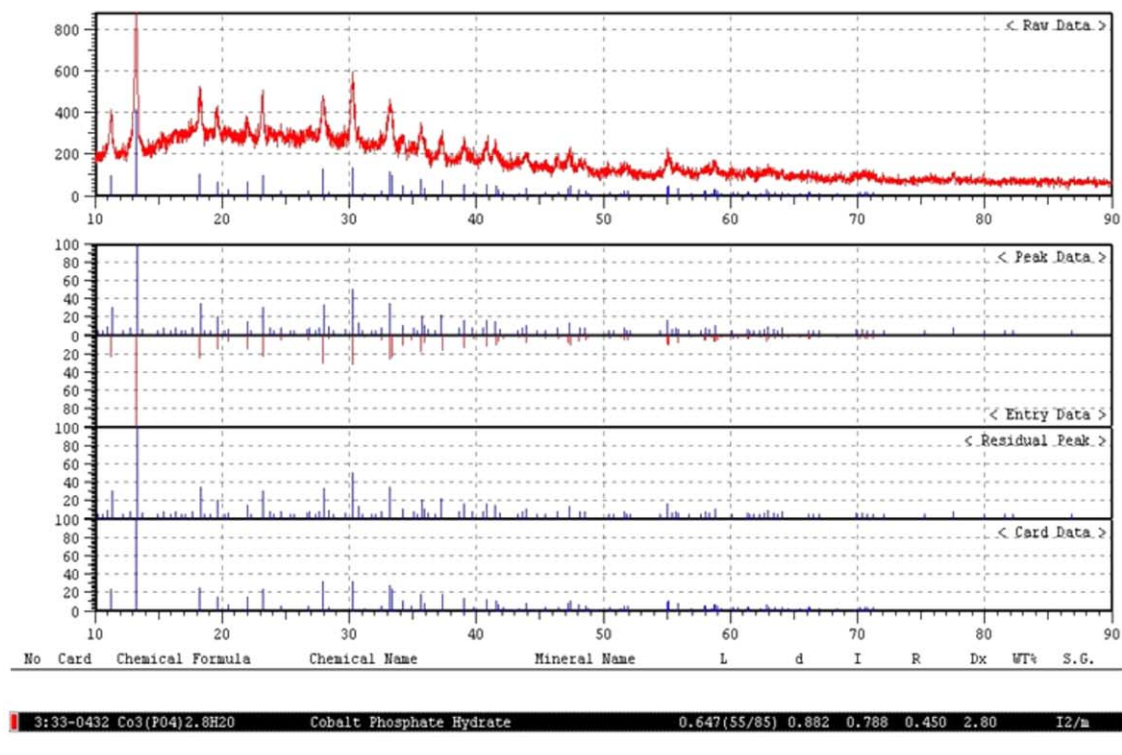
heterogeneous surface of adsorbent as well as multilayer sorption. Equation (6) is used to calculate the constants shown in Table II. As seen from Table II, regression coefficients from the Freundlich isotherm are lower than the Langmuir isotherm. Whereas, on the other hand, hydrogels give the best results according to Langmuir isotherms, poly(DMAPMAm/IA (5 mg)) hydrogel shows the best conformity to Langmuir isotherm when we take into account all pH solutions ( $R^2 = 1.000$  obtained for pH 5 solution).

### Desorption Studies

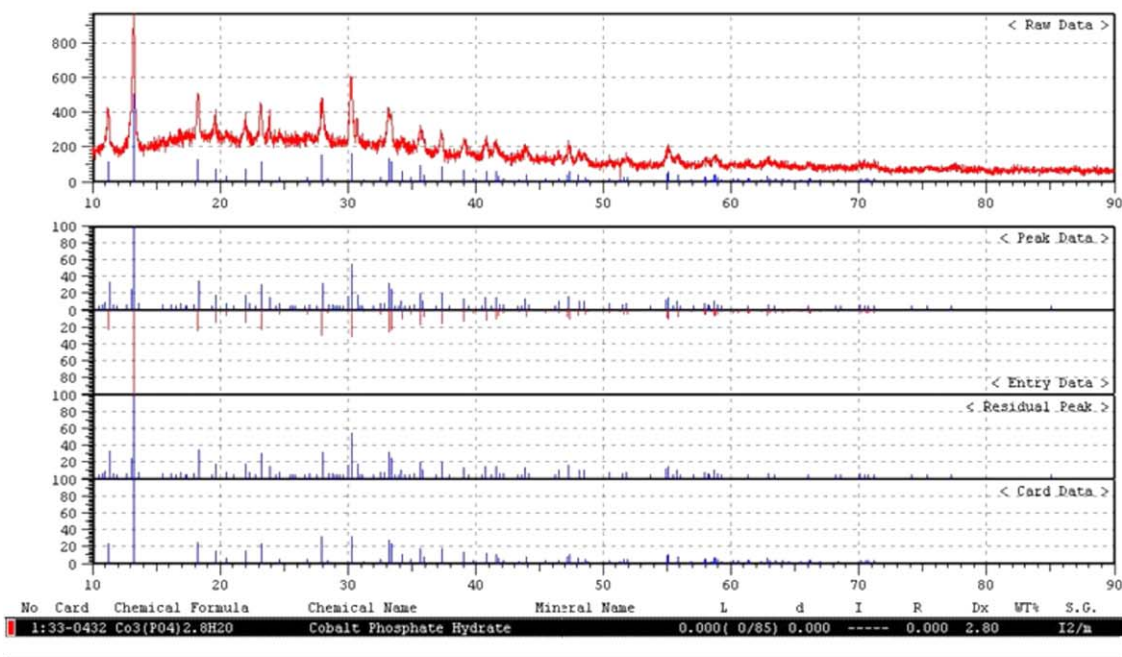
The aim of the desorption experiments is to evaluate the reusability of hydrogels. At first,  $\text{Co}^{2+}$  ions adsorbed hydrogels have been put back to the same pH environment in which metal ion adsorption takes place. It has been revealed that desorption does not occur when the solutions are examined by using UV-Vis Spectrophotometer. Changing the pH of the media has not been enough to release ions since cobalt ions strongly interact with the gels. As a result of these experiments, it has been understood that desorption process will be performed with an agent such as EDTA. EDTA is a multidentate ligand, which is represented by the formula  $\text{H}_4\text{Y}$  in general. Depending on the pH, EDTA will be present in different forms including  $\text{H}_4\text{Y}$ ,  $\text{H}_3\text{Y}^-$ ,  $\text{H}_2\text{Y}^{2-}$ ,  $\text{HY}^{3-}$ , and  $\text{Y}^{4-}$ . When EDTA reacts with a metal ion, the hydrogen attached to the carboxylate groups must be removed. If the media is strongly basic, this hydrogen is removed through reaction with hydroxide ion and EDTA turns into  $\text{Y}^{4-}$  form. The reaction occurred between  $\text{Y}^{4-}$  and metal ion ( $\text{M}^{n+}$ ) is seen below.







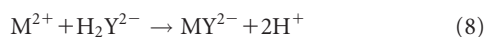
(a)



(b)

**Figure 9.** XRD patterns of Co<sup>2+</sup> adsorbed hydrogels: (a) polyDMAPMAm, and (b) poly(DMAPMAm/IA (10 mg)) exposed to 1000 mg/L aqueous Co<sup>2+</sup> solution. [Color figure can be viewed in the online issue, which is available at [wileyonlinelibrary.com](http://wileyonlinelibrary.com).]

In more acidic solutions, metal ions must be able to displace the hydrogen as shown below if a complex is to be formed.



Consequently, the solution acidity can be adjusted to regulate the reactivity of EDTA toward metal ions to be desired.<sup>51</sup> It is because of that 0.1M EDTA solution was used for desorption experiments. A high tendency to form of a complex with

**Table II.** Parameters of Adsorption Isotherm of Co<sup>2+</sup> on Gels

Co <sup>2+</sup> -hydrogel	Experimental $q_e$	Langmuir data			Freundlich data		
		$X_m$	$K_L$	Correlation coefficient ( $R^2$ )	$K_F$	$n$	Correlation coefficient ( $R^2$ )
pH 3							
DMAPMAm	200.14	192.31	0.0275	0.974	72.31	6.94	0.761
DMAPMAm/IA (1 mg)	188.37	175.44	0.5590	0.994	76.58	7.47	0.879
DMAPMAm/IA (5 mg)	185.27	169.49	0.3810	0.992	77.91	8.05	0.804
DMAPMAm/IA (10 mg)	192.53	196.08	0.0148	0.961	65.61	6.69	0.778
pH 4							
DMAPMAm	219.46	212.77	0.0726	0.993	-	-	-
DMAPMAm/IA (1 mg)	218.34	222.22	0.0457	0.995	-	-	-
DMAPMAm/IA (5 mg)	209.08	208.33	0.0624	0.995	-	-	-
DMAPMAm/IA (10 mg)	203.22	204.08	0.0581	0.999	81.11	7.00	0.848
pH 5							
DMAPMAm	244.82	238.10	0.0358	0.977	87.98	6.64	0.854
DMAPMAm/IA (1 mg)	229.42	222.22	0.0366	0.984	97.99	8.45	0.930
DMAPMAm/IA (5 mg)	219.68	222.22	0.1010	1.000	99.31	7.45	0.836
DMAPMAm/IA (10 mg)	236.07	227.27	0.0412	0.983	97.01	7.82	0.805

-  $R^2$  values are too low.

organic agents, especially with EDTA ( $K_{Co-EDTA} = 2.0 \times 10^{16}$ ) is observed with some metal ions.<sup>51</sup> The amount of metal ions which are passed from hydrogel to the solution in desorption study has been investigated with respect to time (Figure 10).

When Figure 10 is examined, it is seen that the amount of Co<sup>2+</sup> ions passed to the solution has reached 60% in first 10 min. In the following minutes, there has not seen any certain increase in the release rate. Within approximately 8 days,

**Table III.** Comparison of Co<sup>2+</sup> Ion Adsorption Capacities of Some Adsorbents in the Literature

Adsorbent	$q_e$ (mg/g)	Reference
Poly(N,N-dimethylaminopropyl methacrylamide), (DMAPMAm)	244.82	This study
Almond green hull	45.5	[39]
Poly(2-acrylamido-2-methyl-1-propansulfonic acid), p(AMPS)	101.78	[40] <sup>a</sup>
Magnetic p(AMPS)	110.07	[40] <sup>a</sup>
Calcined modified kaolinite	5.3	[41] <sup>b</sup>
Calcined modified montmorillonite	15.8	[42] <sup>b</sup>
EDTA-modified silica gel	20.0	[43] <sup>c</sup>
DTPA-modified silica gel	16.1	[43] <sup>c</sup>
Black carrot residue	5.35	[44]
ZrO-Montmorillonite	22.8	[45]
ZrO-Kaolinite	9.6	[45]
Activated coir pith	12.82	[46]
Activated carbon prepared from hazelnut shells	13.88	[47] <sup>d</sup>
Multiwalled carbon nanotube-cyclo dextrin polymer	3.89	[48] <sup>e</sup>
Lemon peel	22	[49]
Industrial waste	35	[50]

EDTA, ethylenediaminetetraacetic acid; DTPA, diethylenetriaminepentaacetic acid.

<sup>a</sup> Initial ion concentration: 500 mg/L, approximately 0.2 g dry adsorbents.

<sup>b</sup> Clay 2 g/L; initial metal ion concentration 50 mg/L; pH: Co<sup>2+</sup> 5.8, 303 K

<sup>c</sup> Initial concentration of 10 mg/L were 2 g/L of dose, pH 3, 50 rpm of agitation speed and 4 h of contact time.

<sup>d</sup> pH 6, 303K, particle size 1.00-1.20 mm.

<sup>e</sup> pH 7.0.

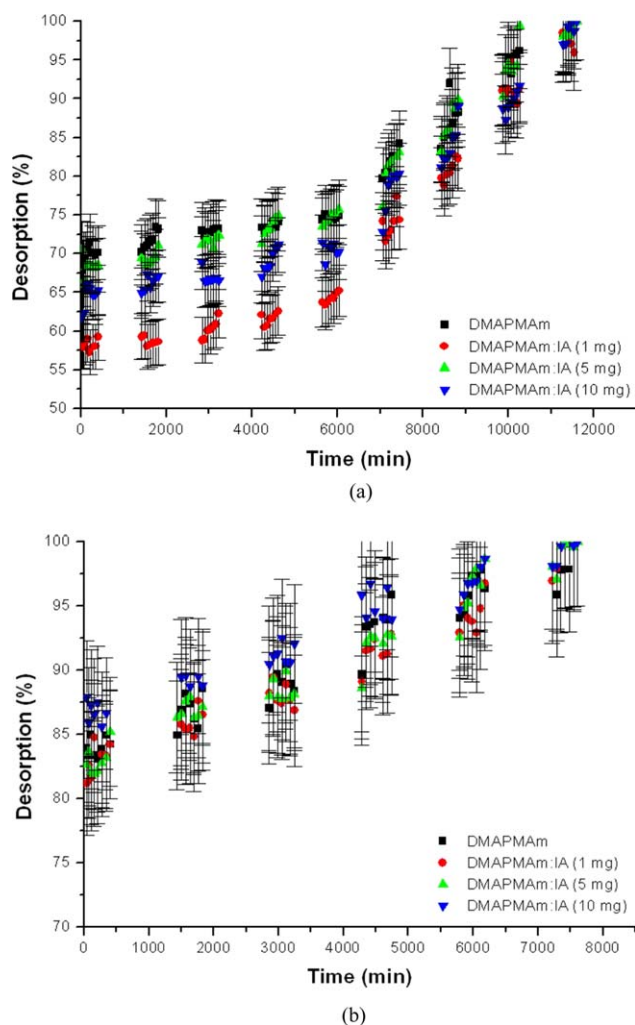
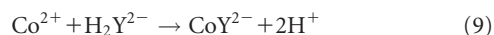


**Figure 10.** Desorption kinetics of Co<sup>2+</sup> adsorbed gels: (a) pH 3 and 0, 1M EDTA solution, and (b) pH 5 and 0, 1M EDTA solution. [Color figure can be viewed in the online issue, which is available at [wileyonlinelibrary.com](http://wileyonlinelibrary.com).]

hydrogels give cobalt ions to form Co-EDTA complex from their bodies to the solution at pH 3 as seen below.



The data in Figure 10(a) presents some differences from Figure 10(b). It is particularly seen that the amount of Co<sup>2+</sup> ions, which are passed to the solution, has reached 80% in first 10 min. Also, a slight increase in the release rate has been seen in the following minutes. Gels give the cobalt ions in their textures to the solution at pH 3 within approximately 8 days. Co<sup>2+</sup> release rate of hydrogels with EDTA solution at pH 5 is higher than that of hydrogels with EDTA solution at pH 3. The regeneration process of the gels in the pH 5 of EDTA solution is completed within less time than the others.

## CONCLUSION

In this study, homopolymer consisting of only DMAPMAM monomer was synthesized while the synthesis of copolymers

was achieved by adding different amounts of IA (1, 5, 10 mg) monomer to DMAPMAM. FTIR, SEM, EDS analyses were performed to characterize these gels. Adsorption studies were performed in the Co<sup>2+</sup> ion solutions having three different pH mediums (pH 3, 4, and 5). When it comes to the maximum capacity values obtained from adsorption experiments by using Co<sup>2+</sup> solutions at pH 5, they have changed between 220 and 245 mg Co<sup>2+</sup>/g dry hydrogel. At the end of the experiments, it has been found that adsorption capacity increases with the increasing of IA content of gels in all studied pHs. Phosphate bands recognized in the FTIR spectra have shown that phosphate groups are adsorbed by the gel surface. In parallel with the analysis of FTIR, P atoms have also been detected as well as Co atoms on the gel surface through EDS analyses. Phosphorous materials containing nutrient feature are present in the industrial, agricultural, and domestic waste water. These waste waters intermingling with surface waters cause eutrophication and thus they threaten the biological life. Especially removal of colloidal structures from the waste waters requires a very difficult and very costly process. From this point of view, behavior of the synthesized polymers against the phosphate groups is very useful. In order to investigate the reusability of gels, release experiments of metal ions from gels, which is desorption studies, have been accomplished by using EDTA solution. While gels give cobalt ions in their textures to the solution at pH 3 within approximately 8 days, gels give cobalt ions in their textures to the solution at pH 5 approximately within 5 days, unlike pH 3.

In addition, synthesized homo and co-polymeric structures have been successfully used in the removal of Co<sup>2+</sup> ions from the aqueous systems and reusability of gels has been shown. However, the study should be extended by doing adsorption experiments of gels with other metal ions.

## ACKNOWLEDGMENTS

The authors gratefully acknowledge the support provided by the Afyon Kocatepe University Coordinating Unit for Scientific Research Projects through the Research Contract No:BAPK-07.FENED.16. The authors also would like to thank Dr. Evren Çubukçu working in the Earth Sciences Application and Research Center/Department of Geological Engineering at Hacettepe University for measurements of SEM-EDS analysis.

## REFERENCES

- Singh, A.; Sharma, P. K.; Garg, V. K.; Garg, G. *Int. J. Pharm. Sci. Rev. Res. (IJPSRR)*, **2010**, *4*, 97.
- Lutolf, M. P.; Raeber, G. P.; Zisch, A. H.; Tirelli, N.; Hubbell, J. A. *Adv. Mater.* **2003**, *15*, 888.
- Ganji, F.; Abdekhodaie, M. J. *Carbohydr. Polym.* **2008**, *74*, 435.
- Hosseinkhani, H.; Hosseinkhani, M.; Khademhosseini, A. *Biomaterials* **2006**, *27*, 5836.
- Kashyap, N.; Kumar, N.; Kumar, M. *Crit. Rev. Ther. Drug* **2005**, *22*, 107.
- Hosseinkhani, H.; Hosseinkhani, M.; Kobayashi, H. J. *Bioact. Compat. Pol.* **2006**, *21*, 277.
- Hosseinkhani, H.; Hosseinkhani, M. *Current Drug Safety* **2009**, *4*, 79.

8. Lee, K. Y.; Mooney, D. J. *Chem. Rev.* **2001**, *10*, 1869.
9. Gao, D.; Xu, H.; Philbert, M. A.; Kopelman, R. *Angew. Chem. Int. Ed.* **2007**, *46*, 2224.
10. Aalaie, J.; Rahmatpour, A.; Vasheghani-Farahani, E. *Polym. Adv. Technol.* **2009**, *20*, 1102.
11. Aalaie, J.; Vasheghani-Farahani, J. E.; Rahmatpour, A.; Semsarzadeh, M. A. *Eur. Polym. J.* **2008**, *44*, 2024.
12. Panahi, R.; Vasheghani-Farahani, E.; Shojaosadati, S. A. *Biochem. Eng. J.* **2007**, *35*, 352.
13. Järup, L. *Brit. Med. Bull.* **2003**, *68*, 167.
14. Srivastava, S.; Goyal, P. *Novel Biomaterials: Decontamination of Toxic Metals from Wastewater*; Springer, Verlag: Berlin, Heidelberg, **2010**, p 21.
15. Yetimoğlu, E. K.; Kahraman, M. V.; Ercan, Ö.; Akdemir, N.; Apohan, K. *React. Funct. Polym.* **2007**, *67*, 451.
16. Behiari, V.; Sotiropoulou, M.; Bokias, G.; Lianos, P. *Colloid Surface A*, **2008**, *312*, 214.
17. Song, L.; Wang, J.; Zheng, Q.; Zhang, Z. *Tsinghua Sci. Technol.* **2008**, *13*, 249.
18. Bayramgil, N. P. *Polym. Degrad. Stab.* **2008**, *93*, 1504.
19. Kaşgöz, H.; Özgümüş, S.; Orbay, M.; *Polymer* **2003**, *44*, 1785.
20. Li, N.; Bai, R. B.; Liu, C. *Langmuir* **2005**, *21*, 11780.
21. Li, N.; Bai, R. B. *Sep. Purif. Technol.* **2005**, *42*, 237.
22. Min, M.; Shen, L.; Hong, G.; Zhu, M.; Zhang, Y.; Wang, X.; Chen, Y.; Hsiao, B. Y.; *Chem. Eng. J.* **2012**, *197*, 88.
23. Li, X. G.; Feng, H.; Huang, M. R. *Chem. Eur. J.* **2010**, *16*, 10113.
24. Lu, Q. F.; Li, X. G.; Huang, M. R. *Chem. Eur. J.* **2007**, *13*, 6009.
25. Vakıflı, A.; Demirel, G. D.; Caykara, T. J. *Appl. Polym. Sci.* **2010**, *117*, 817.
26. Yetimoğlu, E. K.; Kahraman, M. V.; Ercan, Ö.; Akdemir, Z. S.; Apohan, N. K. *React. Funct. Polym.* **2007**, *67*, 451.
27. Coşkun, R.; Soykan, C.; Saçak, M. *React. Funct. Polym.* **2006**, *66*, 599.
28. Çavuş, S.; Gürdağ, G. *Polym. Adv. Technol.* **2008**, *19*, 1209.
29. Krušić, M.; Filipović, J. *Polymer* **2006**, *47*, 148.
30. Çaykara, T.; Birlik, G. *Macromol. Mater. Eng.* **2005**, *290*, 869.
31. Tuncel, A.; Demirci, D.; Patır, S.; Pişkin, E. J. *Appl. Polym. Sci.* **2002**, *84*, 2060.
32. Das, A.; Ray, A. R. J. *Appl. Polym. Sci.* **2008**, *108*, 1273.
33. Karadağ, E. Preparation and swelling characterization of polymeric hydrogel/clay composites containing acrylamide and investigation of their adsorption properties. Ph.D. Thesis, Cumhuriyet University, **1992**.
34. Tomić, S. L. J.; Mičić, M. M.; Filipović, J. M.; Suljovrujić, E. H. *Radiat. Phys. Chem.* **2007**, *76*, 1390.
35. Weast R. C.; *Handbook of Chemistry and Physics*, 53rd ed; The Chemical Rubber Co.: Ohio, **1972**.
36. Butt, H. J.; Graf, K.; Kappl, M. *Physics and Chemistry of Interfaces*; Wiley: VCH GmbH&Co.KGaA, Weinheim, **2003**, p 181.
37. Langmuir, I. *J. Am. Chem. Soc.* **1918**, *40*, 1361.
38. Freundlich, H. *Colloid and Capillary Chemistry*; Methuen: London, **1926**, p 39.
39. Ahmadpoura, A.; Tahmasbic, M.; Bastamic, T. R.; Besharati, J. A. *J. Hazard. Mater.* **2009**, *166*, 925.
40. Ozay, O.; Ekici, S.; Baran, Y.; Aktas, N.; Sahiner, N. *Water Res.* **2009**, *43*, 4403.
41. Bhattacharyya, K. G.; Gupta, S. S. *Appl. Clay Sci.* **2008**, *41*, 1.
42. Bhattacharyya, K. G.; Gupta, S. S. *Appl. Clay Sci.* **2009**, *46*, 216.
43. Repoa, E.; Kurniawana, T. A.; Warcholb, J. K.; Sillanpää, M. E. *J. Hazard. Mater.* **2009**, *171*, 1071.
44. Güzel, F.; Yakut, H.; Topal, G. *J. Hazard. Mater.* **2008**, *153*, 1275.
45. Bhattacharyya, K. G.; Gupta, S. S. *Colloid Surface A* **2008**, *317*, 71.
46. Parab, H.; Joshi, S.; Shenoy, N.; Lali, A.; Sarma, U. S.; Sudersanan, M. *Process Biochem.* **2006**, *41*, 609.
47. Demirbaş, E. *Adsorpt. Sci. Technol.* **2009**, *21*, 951.
48. Mamba, G.; Mbianda, X. Y.; Govender, P. P.; Mamba, B. B.; Krause, R. W. *J. Appl. Sci.* **2010**, *10*, 940.
49. Bhatnagar, A.; Minocha, A. K.; Sillanpää, M. *Biochem. Eng. J.* **2010**, *48*, 181.
50. Bhatnagar, A.; Minocha, A. K.; Jeon, B. H. *Sep. Sci. Technol.* **2007**, *42*, 1255.
51. Skoog, D. A.; West, D. M.; Holler, F. J. *Fundamentals of Analytical Chemistry*, 5th ed.; Saunders College Publishing: USA, **1988**, p 261.